Imperfect-interaction-free entanglement purification on stationary systems for solid quantum repeaters

GUAN-YU WANG,[1,2] QING AI,[3] 🄳 FU-GUO DENG,[3] 🄳 AND BAO-CANG REN[2,*] 🄳

[1]*College of Mathematics and Physics, Beijing University of Chemical Technology, Beijing 100029, China*
[2]*Department of Physics, Capital Normal University, Beijing 100048, China*
[3]*Department of Physics, Applied Optics Beijing Area Major Laboratory, Beijing Normal University, Beijing 100875, China*
[*]*renbaocang@cnu.edu.cn*

Abstract: Solid quantum repeater is a core part in a large-scale quantum network. Entanglement purification, the key technique in a quantum repeater, is used to distill high-quality nonlocal entanglement from an ensemble in a mixed entangled state and to depress the vicious influence on quantum information carriers caused by noise. Here, we present an imperfect-interaction-free entanglement purification on nonlocal electron spins in quantum dots for solid quantum repeaters, using faithful parity check on electron spins. The faithful parity check can make correct judgement on the parity mode without destructing the nonlocal solid entanglement even with the imperfect interaction between a QD embedded inside a microcavity and a circularly polarized photon in the nearly realistic condition. Therefore, the imperfect-interaction-free entanglement purification can prevent the maximally entangled states from being changed into partially entangled ones and guarantee the fidelity of the nonlocal mixed state to a desired one after purification. As this scheme is feasible in the nearly realistic condition with imperfect interaction, the requirements for experimental implementation will be relaxed. These distinctive features make this imperfect-interaction-free entanglement purification have more practical applications in solid quantum repeaters for a large-scale quantum network.

1. Introduction

Quantum entanglement is a key resource in quantum computation and quantum communication, as it provides the tremendous power for speeding up the computation [1–3] and improves security of communication [4–13]. Nonlocal maximal entanglement provides a useful way for establishing quantum communication channels in quantum communication protocols including quantum teleportation [4], quantum dense coding [5,6], quantum key distribution [7,8], quantum secret sharing [9], quantum secure direction communication [10–13], and so on. In the quantum network established by the quantum entanglement, a basic problem for communication between remote nodes is to hold nearly perfect entanglement. Unfortunately, the quality of entanglement between two nodes decreases exponentially with the length of the communication channel due to the decoherence and photon losses in the entanglement storage and distribution processes, which may limit the communication distance to hundreds of kilometres [14]. This bottleneck can be overcome by using the quantum repeater originally proposed by Briegel *et al.* in 1998 [15]. The principle of quantum repeater can be described as follows: In order to generate entanglement between two remote nodes, say quantum memories A and Z, entanglement is first created independently within short elementary links, i.e. between the quantum memories A and B, C and D,. . . , W and X, Y and Z. After entanglement swapping, entanglement is then generated between quantum memories A and D,. . . , W and Z. Through cascading entanglement swapping,

entanglement is generated between the terminal quantum memories *A* and *Z*. In the seminal DLCZ protocol, Duan *et al.* proposed the "from-the-memory" quantum repeater using atomic ensembles as quantum memories [16]. In a quantum repeater, nested entanglement purification [17,18] is an ingredient component to distill high-fidelity entangled states from low-fidelity entangled ones within short elementary links [15,16]. There are two ways for entanglement purification in the "from-the-memory" quantum repeater. One way is to convert the entangled states stored in the quantum memories into entangled photons first [19] and subsequently purify entangled photons [20]. The other way is to directly purify entangled quantum memories.

Quantum stationary systems are usually acted as quantum memories in the network of quantum communication and quantum computation. Diamond nitrogen vacancy centers, atomic ensembles, single trapped ions, and quantum dots (QDs) are frequently-used quantum stationary systems in quantum repeaters [21–33], and many interesting entanglement purification protocols (EPPs) on these quantum stationary systems have been proposed [34–45]. A charged QD is one of the most promising quantum stationary systems playing the role of quantum memory in the quantum network, due to the long coherence time of an electron spin in a QD. The coherence time of an electron spin in a charged QD can maintain $3\mu s$ [46,47], and the relaxation time of an electron spin can reach the order of *ms* [48,49] through the technique of spin echo. Meanwhile, fast preparation of the superposition state of the electron spin [50,51] has been demonstrated, and fast manipulation [52–55] and detection [56] of the electron spin state in a QD have been reported in recent years. Furthermore, in view of realizing a QD embedded in a microcavity (QD-microcavity system) [57,58], the interaction between a QD-microcavity system and a circularly polarized photon has attracted much attention for its applications in quantum information processing [59,60], especially in quantum repeater using QD systems and entanglement purification on electron spins in QDs [31,40].

Since the first EPP proposed by Bennett *et al.* [17], a number of approaches, such as controlled-NOT (CNOT) gate, Toffoli gate, parity check, and hyperentanglement, have been considered to assist completing entanglement purification [20,61–70]. Parity check is an important method which has been used to reserve the two pairs of entangled systems in the same parity mode and discard the ones in the different parity modes. In this method, it is especially important to correctly judge the parity mode with nondestruction on the entangled state. However, using the interaction between a QD-microcavity system and a circularly polarized photon, the parity check is faithful only in specifically ideal conditions, which is difficult to be accomplished. In the realistic experiment, the interaction between a QD-microcavity system and a circularly polarized photon turns imperfect due to the realistic experiment parameters deviate from the specifically ideal ones, and it will lead to an unfaithful parity check, including wrong judgement on the parity mode and destruction on the entangled system. If an unfaithful parity check makes a wrong judgement on the parity mode, the fidelity of the mixed states cannot reach a desired one after purification. Moreover, if an unfaithful parity check has a destruction on the entangled system, the maximally entangled states in the mixed states would be changed into partially entangled states (the detailed information can be found in Sec. 4).

In this paper, we propose an imperfect-interaction-free EPP for QD systems by constructing a faithful parity check in the nearly realistic condition. The faithful parity check has nondestruction on the entangled state and makes correct judgement on the parity mode of an entangled state in the nearly realistic condition. With the faithful parity check, the imperfect-interaction-free EPP can guarantee the desired fidelity of the mixed states and keep the maximally entangled states from being changed into partially entangled ones. Meanwhile, this imperfect-interaction-free EPP relaxes the requirement of experiment techniques as it can be implemented with nonidentical QD-microcavity systems in a nearly realistic condition. Furthermore, this imperfect-interaction-free EPP can be repeated until success, as the faithful parity check is a heralded one, whose failure can be alarmed by the single-photon detector. These distinctive features make this

imperfect-interaction-free EPP for a quantum stationary system more useful in a quantum repeater.

2. Faithful parity check for imperfect-interaction-free EPP

Let us consider the interaction between a QD-microcavity system and a circularly polarized photon first [71]. A singly charged QD (e.g. a self-assembled In(Ga)As QD or a GaAs interfacial QD) inside a double-sided microcavity is shown in Fig. 1(a). Both the bottom and the top distributed Bragg reflectors of the double-sided microcavity are partially reflective with the same reflection coefficients. Meanwhile the microcavity supports both two circularly polarized modes [72–75]. The circularly polarized photon $|R^\uparrow\rangle$ or $|L^\downarrow\rangle$ with $S_z = +1$ is coupled to the dipole transition from the state $|\uparrow\rangle$ to the exciton (X^-) state $|\uparrow\downarrow\Uparrow\rangle$; The circularly polarized photon $|R^\downarrow\rangle$ or $|L^\uparrow\rangle$ with $S_z = -1$ is coupled to the dipole transition from the state $|\downarrow\rangle$ to the exciton (X^-) state $|\downarrow\uparrow\Downarrow\rangle$, as shown in Fig. 1(b). Here, $|\uparrow\rangle$ and $|\downarrow\rangle$ denote the states of the excess electron spin in a QD with $J_z = \pm\frac{1}{2}$, respectively. $|\uparrow\downarrow\Uparrow\rangle$ and $|\downarrow\uparrow\Downarrow\rangle$ denote the states of the exciton consisting of two electrons bound to one heavy hole with $J_z = \pm\frac{3}{2}$, respectively.
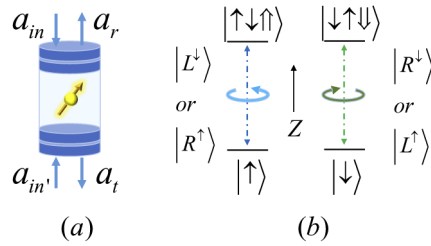

Fig. 1. (a) Schematic diagram for an electron-spin of a QD inside a double-sided optical microcavity. (b) Schematic description of the relevant exciton energy levels and the spin selection rules for dipole transitions of negatively charged excitons. $|R^\uparrow\rangle(|R^\downarrow\rangle)$ and $|L^\uparrow\rangle(|L^\downarrow\rangle)$ represent the right-circularly polarized photon and the left-circularly polarized photon propagating along (against) the normal direction of the cavity Z axis (quantization axis), respectively.

The dynamic process of the interaction between a QD-microcavity system and a circularly polarized photon can be represented by Heisenberg equations of motion for the cavity field operator $\hat{a}$ and the exciton X^- dipole operator $\hat{\sigma}_-$ in the interaction picture [76],

$$
\begin{aligned}
\frac{d\hat{a}}{dt} &= -\left[i(\omega_c - \omega) + \kappa + \frac{\kappa_s}{2}\right]\hat{a} - g\hat{\sigma}_- - \sqrt{\kappa}\hat{a}_{in'} - \sqrt{\kappa}\hat{a}_{in} + \hat{H}, \\
\frac{d\hat{\sigma}_-}{dt} &= -\left[i(\omega_{X^-} - \omega) + \frac{\gamma}{2}\right]\hat{\sigma}_- - g\hat{\sigma}_z\hat{a} + \hat{G},
\end{aligned}
\tag{1}
$$

where ω_c, ω_{X^-}, and ω are the frequencies of the cavity, the X^- transition, and the photon, respectively. g is the coupling strength between the X^- and the microcavity. κ and κ_s are the microcavity-field decay rate and side-leaky rate of microcavity respectively, and γ is the decay rate of exciton dipole. $\hat{H}$ and $\hat{G}$ are the noise operators related to reservoirs. $\hat{a}_{in}$, $\hat{a}_{in'}$, $\hat{a}_r$, and $\hat{a}_t$ are the input and output field operators, which satisfy the boundary relation $\hat{a}_r = \hat{a}_{in} + \sqrt{\kappa}\hat{a}$ and $\hat{a}_t = \hat{a}_{in'} + \sqrt{\kappa}\hat{a}$ [76]. From Eq. (1) and the boundary relation, in the weak excitation approximation, the reflection coefficient r and the transmission coefficient t can be obtained as: [71,77–79]

$$
r = 1 + t, \qquad t = -\frac{\kappa[i(\omega_{X^-} - \omega) + \frac{\gamma}{2}]}{[i(\omega_{X^-} - \omega) + \frac{\gamma}{2}][i(\omega_c - \omega) + \kappa + \frac{\kappa_s}{2}] + g^2}.
\tag{2}
$$

When the QD is decoupled to the microcavity with the coupling strength $g = 0$, the reflection coefficient r_0 and the transmission coefficient t_0 can be written as:

$$r_0 = \frac{i(\omega_c - \omega) + \frac{\kappa_s}{2}}{i(\omega_c - \omega) + \kappa + \frac{\kappa_s}{2}}, \qquad t_0 = -\frac{\kappa}{i(\omega_c - \omega) + \kappa + \frac{\kappa_s}{2}}. \tag{3}$$

If the parameters of the QD-microcavity system and the circularly polarized photon are confined in the specifically ideal condition (i.e. the strong coupling $g > (\kappa, \gamma)$ and the frequency $|\omega - \omega_0| < \kappa$ are satisfied, where $\omega_0 = \omega_c = \omega_{X^-}$), the reflection and transmission coefficients $r_0 \to 0$, $t_0 \to -1$ for the uncoupled cavity and $r \to 1$, $t \to 0$ for the coupled cavity can be obtained, and the interaction between a QD-microcavity system and a circularly polarized photon can be approximately expressed as [71]:

$$\begin{aligned}
&|R^\uparrow \uparrow\rangle \to |L^\downarrow \uparrow\rangle, \quad |L^\downarrow \uparrow\rangle \to |R^\uparrow \uparrow\rangle, \quad |R^\downarrow \uparrow\rangle \to -|R^\downarrow \uparrow\rangle, \quad |L^\uparrow \uparrow\rangle \to -|L^\uparrow \uparrow\rangle, \\
&|R^\downarrow \downarrow\rangle \to |L^\uparrow \downarrow\rangle, \quad |L^\uparrow \downarrow\rangle \to |R^\downarrow \downarrow\rangle, \quad |R^\uparrow \downarrow\rangle \to -|R^\uparrow \downarrow\rangle, \quad |L^\downarrow \downarrow\rangle \to -|L^\downarrow \downarrow\rangle.
\end{aligned} \tag{4}$$

However, when the parameters are not confined in the specifically ideal condition, the interaction between a QD-microcavity system and a circularly polarized photon turns imperfect compared with the ideal one as shown in Eq. (4), and it can be expressed as [71]:

$$\begin{aligned}
|R^\uparrow \uparrow\rangle &\to r|L^\downarrow \uparrow\rangle + t|R^\uparrow \uparrow\rangle, & |L^\downarrow \uparrow\rangle &\to r|R^\uparrow \uparrow\rangle + t|L^\downarrow \uparrow\rangle, \\
|R^\downarrow \uparrow\rangle &\to t_0|R^\downarrow \uparrow\rangle + r_0|L^\uparrow \uparrow\rangle, & |L^\uparrow \uparrow\rangle &\to t_0|L^\uparrow \uparrow\rangle + r_0|R^\downarrow \uparrow\rangle, \\
|R^\downarrow \downarrow\rangle &\to r|L^\uparrow \downarrow\rangle + t|R^\downarrow \downarrow\rangle, & |L^\uparrow \downarrow\rangle &\to r|R^\downarrow \downarrow\rangle + t|L^\uparrow \downarrow\rangle, \\
|R^\uparrow \downarrow\rangle &\to t_0|R^\uparrow \downarrow\rangle + r_0|L^\downarrow \downarrow\rangle, & |L^\downarrow \downarrow\rangle &\to t_0|L^\downarrow \downarrow\rangle + r_0|R^\uparrow \downarrow\rangle.
\end{aligned} \tag{5}$$

The faithful parity check which can make correct judgement on the parity mode without destruction on the entangled states is constructed with a circuit unit based on the imperfect interaction between a QD-microcavity system and a circularly polarized photon as shown in Eq. (5). The circuit unit consists of a 50:50 beam splitter, some half-wave plates, two mirrors, a single-photon detector, and a QD-microcavity system, as shown in Fig. 2(a).

Suppose an electron spin in a QD embedded in a double-sided microcavity is initialized in the state $|\varphi\rangle_s = \alpha|\uparrow\rangle + \beta|\downarrow\rangle$ with $|\alpha|^2 + |\beta|^2 = 1$. A photon in the right-circularly polarized state $|R\rangle$ is injected into the circuit unit from the input path i. After the photon passes through the circuit unit, the state of the system consisting of the photon and the electron spin in the QD is changed from the state $|\Phi\rangle_0 = |R\rangle(\alpha|\uparrow\rangle + \beta|\downarrow\rangle)$ to the state

$$|\Phi\rangle_1 = D|R\rangle_{i_1}(\alpha|\uparrow\rangle + \beta|\downarrow\rangle) + T|L\rangle_{i_2}(\alpha|\uparrow\rangle - \beta|\downarrow\rangle). \tag{6}$$

Here, $D = \frac{1}{2}(t + r + t_0 + r_0)$ and $T = \frac{1}{2}(t + r - t_0 - r_0)$ are the reflection coefficient and the transmission coefficient of the circuit unit, respectively. If the photon is reflected from the circuit unit with the probability of $|D|^2$, there would be no change of the polarization of the photon and the state of the electron spin in the QD, and the reflected photon will be detected by the single-photon detector. If the photon is transmitted from the circuit unit with the probability of $|T|^2$, the polarization of the photon is flipped and the state of the electron spin in the QD is changed from $|\varphi\rangle_s$ to $|\varphi\rangle'_s = \alpha|\uparrow\rangle - \beta|\downarrow\rangle$. The transmitted photon will be emitted out of the circuit unit from the output path i_2 to the following optical path rather than detected by the single-photon detector. For nonidentical QD-microcavity systems, the reflection (transmission) coefficient D (T) may be different, which is determined by the parameters of the QD-microcavity systems.

To faithfully check the parity mode of the entangled state of two electron spins in two QDs, such as QD_A and QD_C, one injects a right-circularly polarized photon from the left-input port *in*
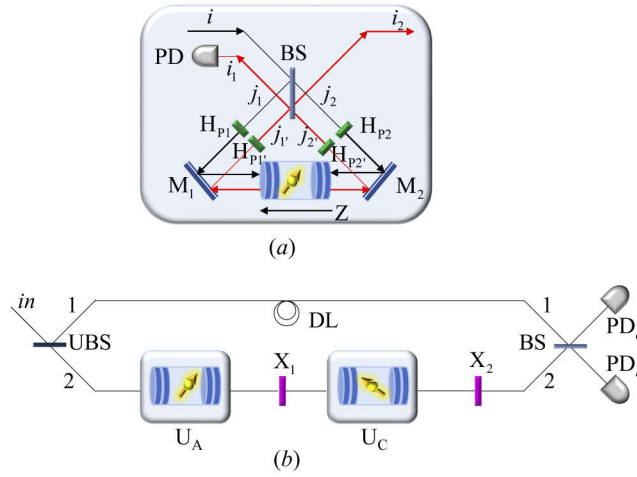
Fig. 2. (a) Schematic diagram for the circuit unit. BS is a 50:50 beam splitter, which performs a spatial-mode Hadamard operation $[|i\rangle \rightarrow \frac{1}{\sqrt{2}}(|j_1\rangle + |j_2\rangle), |i_1\rangle \rightarrow \frac{1}{\sqrt{2}}(|j_{1'}\rangle + |j_{2'}\rangle), |i_2\rangle \rightarrow \frac{1}{\sqrt{2}}(|j_{1'}\rangle - |j_{2'}\rangle)]$ on a photon. $H_{pi(i')(i=1,2)}$ is a half-wave plate, which performs a polarization Hadamard operation $[|R\rangle \rightarrow \frac{1}{\sqrt{2}}(|R\rangle + |L\rangle), |L\rangle \rightarrow \frac{1}{\sqrt{2}}(|R\rangle - |L\rangle)]$ on a photon. $M_{i(i=1,2)}$ is a mirror, and PD is a single-photon detector. (b) Schematic diagram for quantum circuit of the faithful parity check on the electron spins in QDs, say QD_A and QD_C as an example. UBS is an unbalanced beam splitter with the transmission coefficient $\cos\theta = 1/\sqrt{1 + (T_1 T_2)^2}$ and the reflection coefficient $\sin\theta = T_1 T_2/\sqrt{1 + (T_1 T_2)^2}$. BS is a 50:50 beam splitter. $U_{A(C)}$ represents the circuit unit in which the $QD_{A(C)}$-microcavity system is embedded. $X_{i(i=1,2)}$ is a half-wave plate which performs a polarization bit-flip operation $\sigma_x^p = |R\rangle\langle L| + |L\rangle\langle R|$ on the photon. $PD_{i(i=a,b)}$ is a single-photon detector. DL is a time-delay device.

into the quantum circuit of the faithful parity check, as shown in Fig. 2(b). In the process of the parity check, the photon will interact with the first circuit unit U_A consisting of QD_A-microcavity system and the second circuit unit U_C consisting of QD_C-microcavity system, where the two circuit units can be nonidentical and the construction of each one is the same as the one shown in Fig. 2(a). If the initial state of the electron spins in QDs is $|\phi^\pm\rangle = \frac{1}{\sqrt{2}}(|\uparrow\uparrow\rangle \pm |\downarrow\downarrow\rangle)$, after the photon passes through the unbalanced beam splitter UBS, the quantum state of the whole system consisting of the photon and the electron spins in QD_A and QD_C is changed from $|\Psi\rangle_0$ to $|\Psi\rangle_1$. Here,

$$|\Psi\rangle_0 = |R\rangle|\phi^\pm\rangle, \qquad |\Psi\rangle_1 = \frac{1}{\sqrt{1 + (T_1 T_2)^2}}(T_1 T_2|R\rangle_1 + |R\rangle_2)|\phi^\pm\rangle, \qquad (7)$$

where the $|R\rangle_1$ and $|R\rangle_2$ represent the two wave packets split by UBS emerging in path 1 and path 2 respectively, and T_1 and T_2 are equal to the transmission coefficients of the first and the second circuit units respectively. After the wave packet in path 2 passes through the first circuit unit U_A, the whole system consisting of the photon and the electron spins in QDs evolves into

$$|\Psi\rangle_2 = \frac{1}{\sqrt{1 + (T_1 T_2)^2}}\{T_1 T_2|R\rangle_1|\phi^\pm\rangle + [D_1|\phi^\pm\rangle|R\rangle_2 + T_1|\phi^\mp\rangle|L\rangle_2]\}, \qquad (8)$$

where D_1 is the reflection coefficient of the first circuit unit U_A. If there is a click of the single-photon detector in the first circuit unit, say PD_1, the state of the electron spins in QD_A and QD_C is not changed, and the parity mode of the entangled state of electron spins in QD_A and QD_C can be checked through injecting another photon into the quantum circuit for the next round

of parity check. Otherwise, the wave packet in path 2 would pass though the half-wave plate X_1 and the second circuit unit U_C. After the photon passes through the second circuit unit, the state of the whole system is changed into

$$|\Psi\rangle_3 = \frac{1}{\sqrt{1 + (T_1 T_2)^2}} \{T_1 T_2 |R\rangle_1 |\phi^\pm\rangle + T_1 [D_2 |\phi^\mp\rangle |R\rangle_2 + T_2 |\phi^\pm\rangle |L\rangle_2]\}, \qquad (9)$$

where D_2 is the reflection coefficient of the second circuit unit U_C. If there is a click of the single-photon detector in the second circuit unit, say PD_2, the parity mode of the entangled electron spins in QD_A and QD_C can be checked through injecting another photon into the quantum circuit for the next round of parity check after performing an operation $\sigma_z = |\uparrow\rangle\langle\uparrow| - |\downarrow\rangle\langle\downarrow|$ on electron spin in QD_C. Otherwise, the wave packet in path 2 would pass through the half-wave plate X_2, and the state of the whole system becomes

$$|\Psi\rangle_4 = \frac{T_1 T_2}{\sqrt{1 + (T_1 T_2)^2}} (|R\rangle_1 + |R\rangle_2) |\phi^\pm\rangle. \qquad (10)$$

Finally, the two wave packets in path 1 and path 2 reunite at the balanced beam splitter BS, and the final state can be expressed as

$$|\Psi\rangle_{f1} = \sqrt{\frac{2(T_1 T_2)^2}{1 + (T_1 T_2)^2}} |\phi^\pm\rangle |R\rangle_a. \qquad (11)$$

Here, $|R\rangle_a$ represents that the photon triggers the single-photon detector PD_a. Similarly, if the state of the electron spins in QD_A and QD_C is $|\psi^\pm\rangle = \frac{1}{\sqrt{2}}(|\uparrow\downarrow\rangle \pm |\downarrow\uparrow\rangle)$, after the faithful parity check process, as shown in Fig. 2(b), the final state of the system can be expressed as

$$|\Psi\rangle_{f2} = \sqrt{\frac{2(T_1 T_2)^2}{1 + (T_1 T_2)^2}} |\psi^\pm\rangle |R\rangle_b. \qquad (12)$$

Here, $|R\rangle_b$ represents that the photon triggers the single-photon detector PD_b.

In the process of parity check, the single-photon detector PD_1 clicks with a probability of $\frac{D_1^2}{1+(T_1 T_2)^2}$, and the single-photon detector PD_2 clicks with a probability of $\frac{T_1^2 D_2^2}{1+(T_1 T_2)^2}$. The click of PD_1 or PD_2 marks the failure of this round of parity check, and the parity mode of entangled state of the electron spins in QD_A and QD_C can be checked through injecting another photon into the quantum circuit directly (or after an operation σ_z on the electron spin in QD_C in the second circuit unit). That is, the failure of the parity check can be alarmed by the click of PD_1 or PD_2, and the parity check can be repeated until success.

With the faithful parity check as shown in Fig. 2(b), the even-parity states $|\phi^\pm\rangle$ can be distinguished from the odd-parity states $|\psi^\pm\rangle$ by the click of single-photon detector PD_a or PD_b. From the final states in the nearly realistic condition, as shown in Eq. (11) and Eq. (12), one can see that the maximally entangled states $|\phi^\pm\rangle$ and $|\psi^\pm\rangle$ are not changed (such as being destructed into partially entangled states). Meanwhile, one can see that in the nearly realistic condition, there is no wrong judgement being made, as the click of the single-photon detector PD_b (PD_a) does't happen when the pair of entangled electron spins in QDs is in the even-parity states $|\phi^\pm\rangle$ (odd-parity states $|\psi^\pm\rangle$). The only difference between the final states $|\Psi\rangle_{f1}$ ($|\Psi\rangle_{f2}$) in the nearly realistic condition and the ideal final states $|\phi^\pm\rangle|R\rangle_a$ ($|\psi^\pm\rangle|R\rangle_b$) in the specifically ideal condition is an integrate coefficient $\sqrt{\frac{2(T_1 T_2)^2}{1+(T_1 T_2)^2}}$, which only affects the efficiency of the parity check.

3. Imperfect-interaction-free EPP

The four Bell states of a pair of entangled electron spins in two QDs are $|\phi^\pm\rangle = \frac{1}{\sqrt{2}}|\uparrow\uparrow\rangle \pm |\downarrow\downarrow\rangle$ and $|\psi^\pm\rangle = \frac{1}{\sqrt{2}}|\uparrow\downarrow\rangle \pm |\downarrow\uparrow\rangle$. Affected by the environmental noise, bit-flip errors or phase-flip

errors may happen on the entangled systems, which change the maximally entangled state into the mixed state. The phase-flip error can be transformed into the bit-flip error through local Hadamard operations. Here, we discuss imperfect-interaction-free entanglement purification on the QD system in a mixed state with a bit-flip error. To purify the entangled QD system, say QD_A and QD_B, another entangled QD system, say QD_C and QD_D, is needed. The two pairs of entangled electron spins in the QDs are in the same mixed state with the bit-flip error, which can be expressed as

$$\rho_{AB} = F|\phi^+\rangle_{AB}\langle\phi^+| + (1-F)|\psi^+\rangle_{AB}\langle\psi^+|,$$
$$\rho_{CD} = F|\phi^+\rangle_{CD}\langle\phi^+| + (1-F)|\psi^+\rangle_{CD}\langle\psi^+|. \tag{13}$$

Here, F and $1-F$ represent the probabilities of the desired state $|\phi^+\rangle$ and the false state $|\psi^+\rangle$ in the mixed state, respectively. The QDs are shared by two nodes in a quantum network, say Alice and Bob. The QD_A and QD_C are kept by Alice, and the QD_B and QD_D are kept by Bob. The initial state of the system composed of the electron spins in QD_A, QD_B, QD_C, and QD_D is written as $\rho_0 = \rho_{AB} \otimes \rho_{CD}$, which can be seen as a mixture of the pure states $|\phi^+\rangle_{AB} \otimes |\phi^+\rangle_{CD}$, $|\psi^+\rangle_{AB} \otimes |\psi^+\rangle_{CD}$, $|\phi^+\rangle_{AB} \otimes |\psi^+\rangle_{CD}$, and $|\psi^+\rangle_{AB} \otimes |\phi^+\rangle_{CD}$ with the probabilities F^2, $(1-F)^2$, $F(1-F)$, and $F(1-F)$, respectively.

The schematic diagram for our imperfect-interaction-free EPP for QD system is shown in Fig. 3. The first step of our imperfect-interaction-free EPP is to distinguish the states $|\phi^+\rangle_{AB} \otimes |\phi^+\rangle_{CD}$ and $|\psi^+\rangle_{AB} \otimes |\psi^+\rangle_{CD}$ from the states $|\phi^+\rangle_{AB} \otimes |\psi^+\rangle_{CD}$ and $|\psi^+\rangle_{AB} \otimes |\phi^+\rangle_{CD}$. This step can be completed through faithful parity check on the electron spins in QD_A and QD_C by Alice and on the electron spins in QD_B and QD_D by Bob in the nearly realistic condition (the schematic diagram for the faithful parity check is shown in Fig. 2(b)). After Alice performs the faithful parity check on the electron spins in QD_A and QD_C and Bob performs the same operation on the electron spins in QD_B and QD_D, the pure states of the identical two pairs of electron spins in the QDs are classified into two cases based on the results of the parity check.
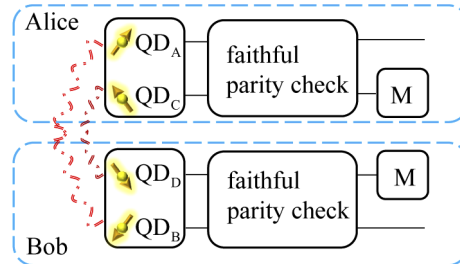

Fig. 3. Schematic diagram for imperfect-interaction-free EPP for QD system. Faithful parity check is the first step of the EPP, which is performed on the electron spins in QD_A and QD_C (QD_B and QD_D) by Alice (Bob). M represents measurement performed on the electron spins in QD_C and QD_D in the orthogonal basis $\{|+\rangle, |-\rangle\}$, which is the second step of the EPP.

In case (1), the electron spins in QD_A and QD_C and the electron spins in QD_B and QD_D are in different parity-mode states, which corresponds to the states $|\phi^+\rangle_{AB}|\psi^+\rangle_{CD}$ and $|\psi^+\rangle_{AB}|\phi^+\rangle_{CD}$. In this case, Alice and Bob cannot identify which pair of entangled electron spins in QDs has the bit-flip error. Therefore, they discard these two pairs of electron spins in QDs.

In case (2), the electron spins in QD_A and QD_C and the electron spins in QD_B and QD_D are in the same parity-mode state, which corresponds to the states $|\phi^+\rangle_{AB}|\phi^+\rangle_{CD}$ and $|\psi^+\rangle_{AB}|\psi^+\rangle_{CD}$. In detail, when the electron spins in QD_A and QD_C and the electron spins in QD_B and QD_D are both in even-parity states, i.e. the single-photon detector PD_a at Alice's side and the single-photon detector PD_a at Bob's side would click respectively in the parity check process, the four electron

spins in the four QDs are projected into a mixed state composed of states $|\Omega\rangle_1$ and $|\Omega\rangle_2$. Here,

$$|\Omega\rangle_1 = \frac{1}{\sqrt{2}}(|\uparrow\uparrow\uparrow\uparrow\rangle + |\downarrow\downarrow\downarrow\downarrow\rangle)_{ABCD}, \qquad |\Omega\rangle_2 = \frac{1}{\sqrt{2}}(|\uparrow\downarrow\uparrow\downarrow\rangle + |\downarrow\uparrow\downarrow\uparrow\rangle)_{ABCD}. \qquad (14)$$

On the contrary, when the electron spins in QD_A and QD_C and the electron spins in QD_B and QD_D are both in odd-parity states, i.e. the single-photon detector PD_b at Alice's side and the single-photon detector PD_b at Bob's side would click respectively in the parity check process, the four electron spins in the four QDs are projected into a mixed state composed of states $|\Omega\rangle_3$ and $|\Omega\rangle_4$. Here,

$$|\Omega\rangle_3 = \frac{1}{\sqrt{2}}(|\uparrow\uparrow\downarrow\downarrow\rangle + |\downarrow\downarrow\uparrow\uparrow\rangle)_{ABCD}, \qquad |\Omega\rangle_4 = \frac{1}{\sqrt{2}}(|\uparrow\downarrow\downarrow\uparrow\rangle + |\downarrow\uparrow\uparrow\downarrow\rangle)_{ABCD}. \qquad (15)$$

The state $|\Omega\rangle_3$ ($|\Omega\rangle_4$) can be transformed into the state $|\Omega\rangle_1$ ($|\Omega\rangle_2$) with bit-flip operations $\sigma_x = |\uparrow\rangle\langle\downarrow| + |\downarrow\rangle\langle\uparrow|$ on both the electron spins in QD_C and QD_D. In this case, Alice and Bob reserve the electron spins in QD_A, QD_C and QD_B, QD_D, and they perform the second step of our imperfect-interaction-free EPP, which is the measurements on the electron spins in QD_C and QD_D in the orthogonal basis $\{|+\rangle = \frac{1}{\sqrt{2}}(|\uparrow\rangle + |\downarrow\rangle), |-\rangle = \frac{1}{\sqrt{2}}(|\uparrow\rangle - |\downarrow\rangle)\}$ as shown in Fig. 3. The evolution can be described as:

$$|\Omega\rangle_1 \Rightarrow \frac{1}{2}[|\phi^+\rangle_{AB}(|++\rangle + |--\rangle)_{CD} + |\phi^-\rangle_{AB}(|+-\rangle + |-+\rangle)_{CD}],$$

$$|\Omega\rangle_2 \Rightarrow \frac{1}{2}[|\psi^+\rangle_{AB}(|++\rangle - |--\rangle)_{CD} + |\psi^-\rangle_{AB}(|-+\rangle - |+-\rangle)_{CD}]. \qquad (16)$$

If the results of the measurements on the electron spins in QD_C and QD_D are $|++\rangle$ or $|--\rangle$, Alice and Bob obtain the mixed state consisting of $|\phi^+\rangle_{AB}$ and $|\psi^+\rangle_{AB}$ directly. If the results of the measurements on the electron spins in QD_C and QD_D are $|+-\rangle$ or $|-+\rangle$, mixed state consisting of $|\phi^+\rangle_{AB}$ and $|\psi^+\rangle_{AB}$ can be obtained with an operation $\sigma_z = |\uparrow\rangle\langle\uparrow| - |\downarrow\rangle\langle\downarrow|$ on the electron spin in QD_B. That is to say, in case (2), Alice and Bob can obtain the mixed states consisting of $|\phi^+\rangle_{AB}$ with the probability of F^2 and $|\psi^+\rangle_{AB}$ with the probability of $(1-F)^2$.

Thus, the first round of our imperfect-interaction-free EPP is completed, and the state of the electron spins in QD_A and QD_B is transformed into

$$\rho'_{AB} = F'|\phi^+\rangle_{AB}\langle\phi^+| + (1-F')|\psi^+\rangle_{AB}\langle\psi^+|. \qquad (17)$$

Here, $F' = \frac{F^2}{F^2+(1-F)^2}$ is the desired fidelity of the final state after the first round of entanglement purification, which is higher than the initial fidelity F when $F > 1/2$. Through iterating the entanglement purification process, the fidelity of the state of the electron spins in QD_A and QD_B can be improved dramatically. The efficiency of one round of entanglement purification is $Y = F^2 + (1-F)^2$.

4. Discussion

The interaction between a QD-microcavity system and a circularly polarized photon is a useful platform in quantum information processing. When the realistic experiment parameters deviate from the specifically ideal ones, the perfect interaction between an artificial atom inside a microcavity (such as QD-microcavity system) and a circularly polarized photon turns into the imperfect one, which results in the wrong judgement on the parity mode and the destruction on the measured entangled state of a parity check in the realistic condition. Let's take the parity check in the entanglement purification protocol using the perfect interaction in the specifically ideal condition [80] as an example to illustrate the bad effect on the parity check in the realistic

condition. In the specifically ideal condition, after the parity check, the states $\frac{1}{\sqrt{2}}(|00\rangle \pm |11\rangle)|\varphi^+\rangle$ and $\frac{1}{\sqrt{2}}(|01\rangle \pm |10\rangle)|\varphi^+\rangle$ of the hybrid system consisting of the measured system and the auxiliary system would be respectively changed into $\frac{1}{\sqrt{2}}(|00\rangle \pm |11\rangle)|\varphi^+\rangle$ and $\frac{1}{\sqrt{2}}(|01\rangle \pm |10\rangle)|\varphi^-\rangle$, which means the final state of the auxiliary system ($|\varphi^+\rangle$ or $|\varphi^-\rangle$) would reflect the parity mode of the measured system (even or odd), and meanwhile the states $\frac{1}{\sqrt{2}}(|00\rangle \pm |11\rangle)$ and $\frac{1}{\sqrt{2}}(|01\rangle \pm |10\rangle)$ of the measured system would not be changed. However, in the realistic condition, the states $\frac{1}{\sqrt{2}}(|00\rangle \pm |11\rangle)|\varphi^+\rangle$ would be changed into $\frac{1}{\sqrt{2}}(|00\rangle \pm \xi|11\rangle)|\varphi^+\rangle \pm \zeta|11\rangle|\varphi^-\rangle$ after the parity check. Obviously, the state of the auxiliary system remains unchanged for correct judgement, and the maximally entangled states $\frac{1}{\sqrt{2}}(|00\rangle \pm |11\rangle)$ of the measured system are destructed into partially entangled states $\frac{1}{\sqrt{2}}(|00\rangle \pm \xi|11\rangle)$. While the state of the auxiliary system is changed for wrong judgement, and the state of the auxiliary system is projected into $\pm\zeta|11\rangle$. For the state $\frac{1}{\sqrt{2}}(|01\rangle \pm |10\rangle)|\varphi^+\rangle$, after the parity check in the realistic condition, it would be changed into $\frac{\epsilon}{\sqrt{2}}(|01\rangle \pm |10\rangle)|\varphi^+\rangle + \frac{\varepsilon}{\sqrt{2}}(|01\rangle \pm |10\rangle)|\varphi^-\rangle$, which means there would be a wrong judgement on the parity mode when the state of the measured system remains unchanged with the possibility of $|\epsilon|^2$. Here, $\xi = \frac{r_0^2+r^2}{2}$, $\zeta = \frac{r_0^2-r^2}{2}$, $\epsilon = -\frac{r_0+r}{2}$, and $\varepsilon = \frac{r-r_0}{2}$ are the functions of the reflection coefficients (r_0 and r) of the circularly polarized photon after interacting with an artificial atom inside a microcavity and they vary with the realistic experiment parameters such as the coupling strength, decay rate, and so on. Therefore, the imperfect interaction due to the realistic experiment parameters would lead a parity check to an unfaithful one.

The unfaithful parity check with the wrong judgement would make the fidelity of the final state lower than the desired one in the entanglement purification process. For example, the parity check makes correct judgements on the parity mode of the states $|\phi^+\rangle_{AB} \otimes |\phi^+\rangle_{CD}$, $|\psi^+\rangle_{AB} \otimes |\psi^+\rangle_{CD}$, and $|\phi^+\rangle_{AB} \otimes |\psi^+\rangle_{CD}$, but it makes a wrong judgement on the parity mode of the state $|\psi^+\rangle_{AB} \otimes |\phi^+\rangle_{CD}$. That is, Alice and Bob may misdeem that the electron spins in QD_A and QD_C and electron spins in QD_B and QD_D are in the same parity-mode states when they are in the state $|\psi^+\rangle_{AB} \otimes |\phi^+\rangle_{CD}$. Then they will reserve the electron spins in QD_A, QD_B, QD_C, and QD_D when they are in the states $|\phi^+\rangle_{AB} \otimes |\phi^+\rangle_{CD}$, $|\psi^+\rangle_{AB} \otimes |\phi^+\rangle_{CD}$, and $|\psi^+\rangle_{AB} \otimes |\psi^+\rangle_{CD}$, but only discard the electron spins in QDs when they are in the state $|\phi^+\rangle_{AB} \otimes |\psi^+\rangle_{CD}$. Thus, after the second step, the first round of the entanglement purification is accomplished and the fidelity of the final state is $F'' = \frac{F^2+0.5F(1-F)}{F^2+(1-F)^2+F(1-F)}$, which is lower than the desired fidelity F' in the condition of $1/2 < F < 1$. We have to admit that there exists a case, in which the parity check makes correct judgements on the parity mode of the states $|\phi^+\rangle_{AB} \otimes |\phi^+\rangle_{CD}$, $|\phi^+\rangle_{AB} \otimes |\psi^+\rangle_{CD}$, and $|\psi^+\rangle_{AB} \otimes |\phi^+\rangle_{CD}$, but it makes a wrong judgement on the parity mode of the state $|\psi^+\rangle_{AB} \otimes |\psi^+\rangle_{CD}$. That is, the electron spins in QD_A, QD_B, QD_C, and QD_D are only reserved when they are in the state $|\phi^+\rangle_{AB} \otimes |\phi^+\rangle_{CD}$. Thus, after the second step, the first round of the entanglement purification is accomplished and the fidelity of the final state is 1. However, this case happens occasionally. More often, the wrong judgement on the parity mode of the state would lead to a lower fidelity of the final state than the desired one. Therefore, making a correct judgements on the parity modes of pure entangled states in the mixed state is of great importance.

Meanwhile, the unfaithful parity check with destruction on the entangled states would also lead the maximally entangled state to the partially entangled one in entanglement purification process. Let us take case (2) of Sec. 3 (i.e. the electron spins in QD_A and QD_C and the electron spins in QD_B and QD_D are both in the even-parity states) as an example to analyze the importance of the nondestruction of a parity check. When the parity check has a destruction on the entangled states in the realistic condition, after the parity check, one of the pure state $|\Omega\rangle_1$ in the mixed state of the four electron spins in QD_A, QD_B, QD_C, and QD_D would be changed into $|\Omega\rangle_1' = (\mu|\uparrow\uparrow\uparrow\uparrow\rangle + \nu|\downarrow\downarrow\downarrow\downarrow\rangle)_{ABCD}$, where $\mu \neq \nu$. Here, μ and ν are quantities varying with the experiment parameters of the QD-microcavity system and the circularly polarized photon in the

realistic condition. Thus, Alice and Bob obtain the states

$$|\Omega\rangle'_1 \Rightarrow \frac{1}{2}[|\phi^+\rangle'_{AB}(|++\rangle + |--\rangle)_{CD} + |\phi^-\rangle'_{AB}(|+-\rangle + |-+\rangle)_{CD}], \qquad (18)$$

where $|\phi^\pm\rangle'_{AB} = (\mu| \uparrow\uparrow\rangle \pm \nu| \downarrow\downarrow\rangle)$. After performing measurements on the electron spins in QD_C and QD_D in the orthogonal basis $\{|+\rangle, |-\rangle\}$, Alice and Bob would obtain the partially entangled states $|\phi^\pm\rangle'_{AB}$ rather than the maximally entangled states $|\phi^\pm\rangle_{AB}$. To distill the partially entangled states $|\phi^\pm\rangle'_{AB}$ to the maximally entangled states $|\phi^\pm\rangle_{AB}$, entanglement concentration is required.

Fortunately, our imperfect-interaction-free EPP can avoid being affected by the imperfect interaction in the nearly realistic condition, as the faithful parity check can make correct judgement on the parity mode of the measured entangled state without destruction. The faithful parity check can correctly identify the parity modes of the pure entangled states in the mixed state of the electron spins in QDs, i.e. correctly distinguish the states $|\phi^+\rangle_{AB} \otimes |\phi^+\rangle_{CD}$ and $|\psi^+\rangle_{AB} \otimes |\psi^+\rangle_{CD}$ from the states $|\phi^+\rangle_{AB} \otimes |\psi^+\rangle_{CD}$ and $|\psi^+\rangle_{AB} \otimes |\phi^+\rangle_{CD}$. Meanwhile, the faithful parity check has nondestruction on the measured entangled states in entanglement purification. Therefore, with our imperfect-interaction-free EPP, the desired fidelity of mixed state can be achieved even in the nearly realistic condition, which can be further improved by iterating the purification process, and maximally entangled states $|\phi^\pm\rangle_{AB}$ and $|\psi^\pm\rangle_{AB}$ would not be changed into partially entangled states, which means the entanglement concentration is not required after purification.

Our imperfect-interaction-free EPP relaxes the strict requirement for two absolutely identical QD-microcavity systems and the high requirement for the QD-microcavity system. Embedding a QD in a microcavity can strengthen the interaction between the circularly polarized photon and the electron spin in a QD, while manufacturing two QD-microcavity systems with absolutely identical experimental parameters is a strict requirement in experiment. In our faithful parity check, the transmission coefficients of the two circuit units T_1 and T_2, varying with the experiment parameters of two QD-microcavity systems, can be different, which means that the faithful parity check could be constructed with nonidentical QD-microcavity systems without affecting the features of nondestruction and correct judgement on the parity mode in the nearly realistic condition. Therefore, the experimental realization of our imperfect-interaction-free EPP doesn't need two absolutely identical QD-microcavity systems. Meanwhile, from Eq. (11) and Eq. (12), one can see that the experiment parameters of the QD-microcavity systems would not affect the features of nondestruction and correct judgement of the faithful parity check in the nearly realistic condition, but only affect the integrate coefficient of the final state after parity check, which determines the efficiency of the parity check. From Eq. (11) and Eq. (12), the efficiency of one round of parity check can be obtained as $\eta = \frac{2(T_1 T_2)^2}{1+(T_1 T_2)^2}$. For simplicity but with no lack of rigor, we plot the efficiency η as a function of $g/(\kappa + \kappa_s)$ and κ_s/κ with $\omega_{X^-} = \omega_C = \omega$ and $\gamma/\kappa = 0.1$ for both two QD-microcavity systems in the two circuit units, as shown in Fig. 4. When $g/(\kappa + \kappa_s) > 1$, the efficiency $\eta > 90.27\%$ and $\eta > 74.05\%$ can be obtained with the cases $\kappa_s/\kappa = 0$ and $\kappa_s/\kappa = 0.2$ respectively. When $g/(\kappa + \kappa_s)$ is improved to 2, the efficiency $\eta = 93.92\%$ and $\eta = 76.70\%$ can be obtained with the cases $\kappa_s/\kappa = 0$ and $\kappa_s/\kappa = 0.2$ respectively. One can see that, utilizing the imperfect interaction in the nearly realistic condition, a faithful parity check is constructed with nearly unity fidelity and the efficiency of it is still acceptable compared with the previous works, the reason of which is that we only transfer the imperfect interaction into a heralded failure by the single photon detectors in the circuit units but not decrease the effective interaction which can be used to assist in completing the parity check.

The interaction between the QD-microcavity system and the circularly polarized photon is utilized to construct the faithful parity check in our imperfect-interaction-free EPP. The experiment parameters of the QD-microcavity system and the single photon would only influence the interaction between the QD-microcavity system and the circularly polarized photon, but not influence the features of nondestruction and correct judgement of our faithful parity check in the
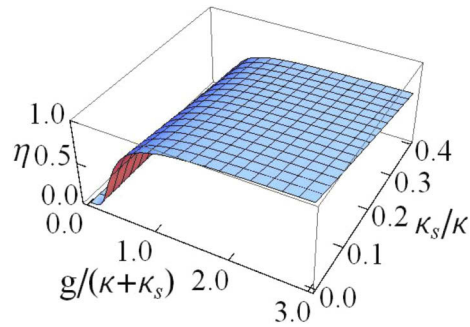
Fig. 4. The efficiency of the faithful parity check vs $g/(\kappa + \kappa_s)$ and κ_s/κ with $\omega_{X^-} = \omega_C = \omega$ and $\gamma/\kappa = 0.1$.

nearly realistic condition. In a more generally realistic condition, the interaction between the QD-microcavity system and the circularly polarized photon could be decreased by a factor of $[1 - exp(-\tau/\Gamma)]$ due to the dephasing of the electron spin in the QD. However, this influence on the features of nondestruction and correct judgement of our faithful parity check can be neglected as an electron spin coherence time $\Gamma \simeq 2.6\mu s$ [81] has been experimentally achieved and the cavity photon time $\tau = 4.5ns$ [82] is available. Imperfect optical selection induced by heavy hole mixing would also affect the features of nondestruction and correct judgement of our faithful parity check a little. Fortunately, this imperfect mixing can be suppressed by engineering the shape and the size of QDs or by choosing the appropriate types of QDs [83]. Overall, even taking the realistic condition into account, the faithful parity check can also remain the features of nondestruction and correct judgement.

Our imperfect-interaction-free EPP works in a repeat-until-success pattern. In our EPP, an auxiliary circularly polarized photon is used to assist in accomplishing our faithful parity check. According to the click of the single-photon detector PD_a or PD_b at the out-put port of the circuit of the faithful parity check, the parity mode of the entangled state can be known. Meanwhile, due to the experiment parameters of the QD-microcavity system and the circularly polarized photon in the realistic condition would deviate from the ones in the specifically ideal condition, there is a possibility that the parity check fails. Fortunately, the failure of the parity check can be alarmed by the click of the single-photon detector in the first circuit unit or the one in the second circuit unit. In this case, the parity mode of the entangled QD systems can be checked through injecting another circularly polarized photon. Therefore, the faithful parity check is a heralded one and the imperfect-interaction-free EPP can be repeated until success.

5. Summary

In conclusion, we propose an imperfect-interaction-free EPP for QD system based on faithful parity check, which can make a correct judgement on the parity mode and have no destruction on the entangled state in the nearly realistic condition. Our imperfect-interaction-free EPP can guarantee the fidelity of the mixed state to a desired one and keep the maximally entangled states in the mixed states from being destructed into partially entangled ones even in the nearly realistic condition. Meanwhile, our imperfect-interaction-free EPP relaxes the strict requirement for two absolutely identical QD-microcavity systems and the high requirement for the QD-microcavity system. In addition, our imperfect-interaction-free EPP can be repeated until success with the heralded function of faithful parity check, where the failure can be alarmed by the single-photon detector. These distinctive features make this imperfect-interaction-free EPP for quantum stationary systems have more practical applications in solid quantum repeaters for a large-scale quantum network.

Funding

Disclosures

The authors declare no conflicts of interest.

References

1. M. A. Nielsen and I. L. Chuang, *Quantum computation and quantum information* (Cambridge University, 2000).
2. A. Ekert and R. Jozsa, "Quantum computation and Shor's factoring algorithm," Rev. Mod. Phys. **68**(3), 733–753 (1996).
3. R. Raussendorf and H. J. Briegel, "A one-way quantum computer," Phys. Rev. Lett. **86**(22), 5188–5191 (2001).
4. C. H. Bennett, G. Brassard, C. Crepeau, R. Jozsa, A. Peres, and W. K. Wootters, "Teleporting an unknown quantum state via dual classical and Einstein-Podolsky-Rosen channels," Phys. Rev. Lett. **70**(13), 1895–1899 (1993).
5. C. H. Bennett and S. J. Wiesner, "Communication via one- and two-particle operators on Einstein-Podolsky-Rosen states," Phys. Rev. Lett. **69**(20), 2881–2884 (1992).
6. X. S. Liu, G. L. Long, D. M. Tong, and F. Li, "General scheme for superdense coding between multiparties," Phys. Rev. A **65**(2), 022304 (2002).
7. A. K. Ekert, "Quantum cryptography based on Bell's theorem," Phys. Rev. Lett. **67**(6), 661–663 (1991).
8. C. H. Bennett, G. Brassard, and N. D. Mermin, "Quantum cryptography without Bell's theorem," Phys. Rev. Lett. **68**(5), 557–559 (1992).
9. M. Hillery, V. Bužek, and A. Berthiaume, "Quantum secret sharing," Phys. Rev. A **59**(3), 1829–1834 (1999).
10. G. L. Long and X. S. Liu, "Theoretically efficient high-capacity quantum-key-distribution scheme," Phys. Rev. A **65**(3), 032302 (2002).
11. F. G. Deng, G. L. Long, and X. S. Liu, "Two-step quantum direct communication protocol using the Einstein-Podolsky-Rosen pair block," Phys. Rev. A **68**(4), 042317 (2003).
12. Z. R. Zhou, Y. B. Sheng, P. H. Niu, L. G. Yin, G. L. Long, and L. Hanzou, "Measurement-device-independent quantum secure direct communication," Sci. China: Phys., Mech. Astron. **63**(3), 230362 (2020).
13. R. He and M. J. G J. W. Wu, "A quantum secure direct communication protocol using entangled beam pairs," EPL **127**(5), 50006 (2019).
14. N. Sangouard, C. Simon, H. d. Riedmatten, and N. Gisin, "Quantum repeaters based on atomic ensembles and linear optics," Rev. Mod. Phys. **83**(1), 33–80 (2011).
15. H. J. Briegel, W. Dür, J. I. Cirac, and P. Zoller, "Quantum repeaters: the role of imperfect local operations in quantum communication," Phys. Rev. Lett. **81**(26), 5932–5935 (1998).
16. L. M. Duan, M. D. Lukin, J. I. Cirac, and P. Zoller, "Long-distance quantum communication with atomic ensembles and linear optics," Nature **414**(6862), 413–418 (2001).
17. C. H. Bennett, G. Brassard, S. Popescu, B. Schumacher, J. A. Smolin, and W. K. Wootters, "Purification of noisy entanglement and faithful teleportation via noisy channels," Phys. Rev. Lett. **76**(5), 722–725 (1996).
18. L. K. Chen, H. L. Yong, P. Xu, X. C. Yao, T. Xiang, Z. D. Li, C. Liu, H. Lu, N. L. Liu, L. Li, T. Yang, C. Z. Peng, B. Zhao, Y. A. Chen, and J. W. Pan, "Experimental nested purification for a linear optical quantum repeater," Nat. Photonics **11**(11), 695–699 (2017).
19. Z. B. Chen, B. Zhao, Y. A. Chen, J. Schmiedmayer, and J. W. Pan, "Fault-tolerant quantum repeater with atomic ensembles and linear optics," Phys. Rev. A **76**(2), 022329 (2007).
20. J. W. Pan, S. Gasparoni, R. Ursin, G. Weihs, and A. Zellinger, "Experimental entanglement purification of arbitrary unknown states," Nature **423**(6938), 417–422 (2003).
21. L. Childress, J. M. Taylor, A. S. Sørensen, and M. D. Lukin, "Fault-tolerant quantum communication based on solid-state photon emitters," Phys. Rev. Lett. **96**(7), 070504 (2006).
22. K. Nemoto, M. Trupke, S. J. Devitt, A. M. Stephens, B. Scharfenberger, K. Buczak, T. Nöbauer, M. S. Everitt, J. Schmiedmayer, and W. J. Munro, "Photonic architecture for scalable quantum information processing in diamond," Phys. Rev. X **4**(3), 031022 (2014).
23. B. Zhao, Z. B. Chen, Y. A. Chen, J. Schmiedmayer, and J. W. Pan, "Robust creation of entanglement between remote memory qubits," Phys. Rev. Lett. **98**(24), 240502 (2007).
24. S. Chen, Y. A. Chen, B. Zhao, Z. S. Yuan, J. Schmiedmayer, and J. W. Pan, "Demonstration of a stable atom-photon entanglement source for quantum repeaters," Phys. Rev. Lett. **99**(18), 180505 (2007).
25. N. Sangouard, C. Simon, H. de Riedmatten, and N. Gisin, "Quantum repeaters based on atomic ensembles and linear optics," Rev. Mod. Phys. **83**(1), 33–80 (2011).
26. N. Sangouard, R. Dubessy, and C. Simon, "Quantum repeaters based on single trapped ions," Phys. Rev. A **79**(4), 042340 (2009).
27. E. Waks and J. Vuckovic, "Dipole induced transparency in drop-filter cavity-waveguide systems," Phys. Rev. Lett. **96**(15), 153601 (2006).

28. C. Simon, Y. M. Niquet, X. Caillet, J. Eymery, J. P. Poizat, and J. M. Gérard, "Quantum communication with quantum dot spins," Phys. Rev. B **75**(8), 081302 (2007).

29. T. J. Wang, S. Y. Song, and G. L. Long, "Quantum repeater based on spatial entanglement of photons and quantum-dot spins in optical microcavities," Phys. Rev. A **85**(6), 062311 (2012).

30. C. Jones, K. D. Greve, and Y. Yamamoto, "A high-speed optical link to entangle quantum dots," arXiv:1310.4609 (2013).

31. T. Li, G. J. Yang, and F. G. Deng, "Heralded quantum repeater for a quantum communication network based on quantum dots embedded in optical microcavities," Phys. Rev. A **93**(1), 012302 (2016).

32. J. Z. Bernád, "Hybrid quantum repeater based on resonant qubit-field interactions," Phys. Rev. A **96**(5), 052329 (2017).

33. T. Li, A. Miranowicz, X. Hu, K. Xia, and F. Nori, "Quantum memory and gates using a Λ-type quantum emitter coupled to a chiral waveguide," Phys. Rev. A **97**(6), 062318 (2018).

34. M. Yang, W. Song, and Z. L. Cao, "Entanglement purification for arbitrary unknown ionic states via linear optics," Phys. Rev. A **71**(1), 012308 (2005).

35. C. D. Ogden, M. Paternostro, and M. S. Kim, "Concentration and purification of entanglement for qubit systems with ancillary cavity fields," Phys. Rev. A **75**(4), 042325 (2007).

36. C. Cong, C. Wang, L. Y. He, and R. Zhang, "Atomic entanglement purification and concentration using coherent state input-output process in low-Q cavity QED regime," Opt. Express **21**(4), 4093–4105 (2013).

37. T. Li, G. J. Yang, and F. G. Deng, "Entanglement distillation for quantum communication network with atomic-ensemble memories," Opt. Express **22**(20), 23897–23911 (2014).

38. R. Reichle, D. Leibfried, E. Knill, J. Britton, R. B. Blakestad, J. D. Jost, C. Langer, R. Ozeri, S. Seidelin, and D. J. Wineland, "Experimental purification of two-atom entanglement," Nature **443**(7113), 838–841 (2006).

39. X. L. Feng, L. C. Kwek, and C. H. Oh, "Electronic entanglement purification scheme enhanced by charge detections," Phys. Rev. A **71**(6), 064301 (2005).

40. C. Wang, Y. Zhang, and G. S. Jin, "Entanglement purification and concentration of electron-spin entangled states using quantum-dot spins in optical microcavities," Phys. Rev. A **84**(3), 032307 (2011).

41. W. C. Gao, C. Cao, T. J. Wang, and C. Wang, "Efficient purification and concentration for Lambda-type three-level entangled quantum dots using non-reciprocal microresonators," Quantum Inf. Process. **16**(8), 182 (2017).

42. N. Kalb, A. A. Reiserer, P. C. Humphreys, J. J. W. Bakermans, S. J. Kamerling, N. H. Nickerson, S. C. Benjamin, D. J. Twitchen, M. Markham, and R. Hanson, "Entanglement distillation between solid-state quantum network nodes," Science **356**(6341), 928–932 (2017).

43. R. Wang, T. J. Wang, and C. Wang, "Entanglement purification and concentration based on hybrid spin entangled states of separate nitrogen-vacancy centers," EPL **126**(4), 40006 (2019).

44. G. Y. Wang and G. L. Long, "Entanglement purification for memory nodes in a quantum network," Sci. China: Phys., Mech. Astron. **63**(2), 220311 (2020).

45. S. M. Hein, C. Aron, and H. E. Türeci, "Purification and switching protocols for dissipatively stabilized entangled qubit states," Phys. Rev. A **93**(6), 062331 (2016).

46. J. R. Petta, A. C. Johnson, J. M. Taylor, E. A. Laird, A. Yacoby, M. D. Lukin, C. M. Marcus, M. P. Hanson, and A. C. Gossard, "Coherent manipulation of coupled electron spins in semiconductor quantum dots," Science **309**(5744), 2180–2184 (2005).

47. A. Greilich, D. R. Yakovlev, A. Shabaev, A. L. Efros, I. A. Yugova, R. Oulton, V. Stavarache, D. Reuter, A. Wieck, and M. Bayer, "Mode locking of electron spin coherences in singly charged quantum dots," Science **313**(5785), 341–345 (2006).

48. J. M. Elzerman, R. Hanson, L. H. Willems van Beveren, B. Witkamp, L. M. K. Vandersypen, and L. P. Kouwenhoven, "Single-shot read-out of an individual electron spin in a quantum dot," Nature **430**(6998), 431–435 (2004).

49. M. Kroutvar, Y. Ducommun, D. Heiss, M. Bichler, D. Schuh, G. Abstreiter, and J. J. Finley, "Optically programmable electron spin memory using semiconductor quantum dots," Nature **432**(7013), 81–84 (2004).

50. M. Atatüre, J. Dreiser, A. Badolato, A. Högele, K. Karrai, and A. Imamoglu, "Quantum-dot spin-state preparation with near-unity fidelity," Science **312**(5773), 551–553 (2006).

51. M. Atatüre, J. Dreiser, A. Badolato, and A. Imamoglu, "Observation of Faraday rotation from a single confined spin," Nat. Phys. **3**(2), 101–106 (2007).

52. J. Berezovsky, M. H. Mikkelsen, N. G. Stoltz, L. A. Coldren, and D. D. Awschalom, "Picosecond coherent optical manipulation of a single electron spin in a quantum dot," Science **320**(5874), 349–352 (2008).

53. D. Press, T. D. Ladd, B. Y. Zhang, and Y. Yamamoto, "Complete quantum control of a single quantum dot spin using ultrafast optical pulses," Nature **456**(7219), 218–221 (2008).

54. J. A. Gupta, R. Knobel, N. Samarth, and D. D. Awschalom, "Ultrafast manipulation of electron spin coherence," Science **292**(5526), 2458–2461 (2001).

55. P. C. Chen, C. Piermarocchi, L. J. Sham, D. Gammon, and D. G. Steel, "Theory of quantum optical control of a single spin in a quantum dot," Phys. Rev. B **69**(7), 075320 (2004).

56. R. Hanson, L. H. Willems van Beveren, I. T. Vink, J. M. Elzerman, W. J. M. Naber, F. H. L. Koppens, L. P. Kouwenhoven, and L. M. K. Vandersypen, "Single-shot readout of electron spin states in a quantum dot using spin-dependent tunnel rates," Phys. Rev. Lett. **94**(19), 196802 (2005).

57. T. Yoshie, A. Scherer, J. Hendrickson, G. Khitrova, H. M. Gibbs, G. Rupper, C. Ell, O. B. Shchekin, and D. G. Deppe, "Vacuum Rabi splitting with a single quantum dot in a photonic crystal nanocavity," Nature **432**(7014), 200–203 (2004).

58. H. J. Chen, "Auxiliary-cavity-assisted vacuum rabi splitting of a semiconductor quantum dot in a photonic crystal nanocavity," Photonics Res. **6**(12), 1171–9125 (2018).

59. T. Li and F. G. Deng, "Error-rejecting quantum computing with solid-state spins assisted by low-Q optical microcavities," Phys. Rev. A **94**(6), 062310 (2016).

60. T. Li, Z. Wang, and K. Y. Xia, "Multipartite quantum entanglement creation for distant stationary systems," Opt. Express **28**(2), 1316–1329 (2020).

61. D. Deutsch, A. Ekert, R. Jozsa, C. Macchiavello, S. Popescu, and A. Sanpera, "Quantum privacy amplification and the security of quantum cryptography over noisy channels," Phys. Rev. Lett. **77**(13), 2818–2821 (1996).

62. M. Murao, M. B. Plenio, S. Popescu, V. Vedral, and P. L. Knight, "Multiparticle entanglement purification protocols," Phys. Rev. A **57**(6), R4075–R4078 (1998).

63. J. W. Pan, C. Simon, Č. Brukner, and A. Zeilinger, "Entanglement purification for quantum communication," Nature **410**(6832), 1067–1070 (2001).

64. C. Simon and J. W. Pan, "Polarization entanglement purification using spatial entanglement," Phys. Rev. Lett. **89**(25), 257901 (2002).

65. X. L. Feng, S. Q. Gong, and Z. Z. Xu, "Entanglement purification via controlled-controlled-NOT operations," Phys. Lett. A **271**(1-2), 44–47 (2000).

66. Y. B. Sheng, F. G. Deng, and H. Y. Zhou, "Efficient polarization-entanglement purification based on parametric down-conversion sources with cross-Kerr non-linearity," Phys. Rev. A **77**(4), 042308 (2008).

67. Y. B. Sheng and F. G. Deng, "Deterministic entanglement purification and complete nonlocal Bell-state analysis with hyperentanglement," Phys. Rev. A **81**(3), 032307 (2010).

68. H. Zhan, Q. Liu, X. S. Xu, J. Xiong, A. Alsaedi, T. Hayat, and F. G. Deng, "Polarization entanglement purification of nonlocal microwave photons based on the cross-Kerr effect in circuit QED," Phys. Rev. A **96**(5), 052330 (2017).

69. L. Zhou, W. Zhong, and Y. B. Sheng, "Purification of the residual entanglement," Opt. Express **28**(2), 2291–2301 (2020).

70. F. F. Du, Y. T. Liu, Z. R. Shi, Y. X. Liang, J. Tang, and J. Liu, "Efficient hyperentanglement purification for three-photon systems with the fidelity-robust quantum gates and hyperentanglement link," Opt. Express **27**(19), 27046–27061 (2019).

71. C. Y. Hu, W. J. Munro, J. L. O'Brien, and J. G. Rarity, "Proposed entanglement beam splitter using a quantum-dot spin in a double-sided optical microcavity," Phys. Rev. B **80**(20), 205326 (2009).

72. I. J. Luxmoore, E. D. Ahmadi, B. J. Luxmoore, N. A. Wasley, A. I. Tartakovskii, M. Hugues, M. S. Skolnick, and A. M. Fox, "Restoring mode degeneracy in H1 photonic crystal cavities by uniaxial strain tuning," Appl. Phys. Lett. **100**(12), 121116 (2012).

73. C. Bonato, E. van Nieuwenburg, J. Gudat, S. Thon, H. Kim, M. P. van Exter, and D. Bouwmeester, "Strain tuning of quantum dot optical transitions via laser-induced surface defects," Phys. Rev. B **84**(7), 075306 (2011).

74. K. Hennessy, C. Högerle, E. Hu, A. Badolato, and A. Imamoğlu, "Tuning photonic nanocavities by atomic force microscope nano-oxidation," Appl. Phys. Lett. **89**(4), 041118 (2006).

75. Y. Eto, A. Noguchi, P. Zhang, M. Ueda, and M. Kozuma, "Projective measurement of a single nuclear spin qubit by using two-mode cavity QED," Phys. Rev. Lett. **106**(16), 160501 (2011).

76. D. F. Walls and G. J. Milburn, *Quantum Optics* (Springer-Verlag, 1994).

77. E. Waks and J. Vuckovic, "Dispersive properties and large Kerr nonlinearities using dipole-induced transparency in a single-sided cavity," Phys. Rev. A **73**(4), 041803 (2006).

78. C. Y. Hu, A. Young, J. L. O'Brien, W. J. Munro, and J. G. Rarity, "Giant optical Faraday rotation induced by a single-electron spin in a quantum dot: Applications to entangling remote spins via a single photon," Phys. Rev. B **78**(8), 085307 (2008).

79. J. H. An, M. Feng, and C. H. Oh, "Quantum-information processing with a single photon by an input-output process with respect to low-Q cavities," Phys. Rev. A **79**(3), 032303 (2009).

80. G. Y. Wang, Q. Liu, and F. G. Deng, "Hyperentanglement purification for two-photon six-qubit quantum systems," Phys. Rev. A **94**(3), 032319 (2016).

81. D. Press, K. D. Greve, P. L. McMahon, T. D. Ladd, B. Friess, C. Schneider, M. Kamp, S. Höfling, A. Forchel, and Y. Yamamoto, "Ultrafast optical spin echo in a single quantum dot," Nat. Photonics **4**(6), 367–370 (2010).

82. C. Y. Hu and J. G. Rarity, "Loss-resistant state teleportation and entanglement swapping using a quantum-dot spin in an optical microcavity," Phys. Rev. B **83**(11), 115303 (2011).

83. G. Bester, S. Nair, and A. Zunger, "Pseudopotential calculation of the excitonic fine structure of million-atom self-assembled $In_{1-x}Ga_xAs/GaAs$ quantum dots," Phys. Rev. B **67**(16), 161306 (2003).